NON-PARABOLIC INTERFACE MOTION FOR THE ONE-DIMENSIONAL STEFAN PROBLEM
Neumann Boundary Conditions

by

Jose A. OTERO*, Ernesto M. HERNANDEZ, Ruben D. SANTIAGO, Raul MARTINEZ, Francisco CASTILLO, and Joaquin E. OSEGUERA

Monterrey Institute of Technology and Higher Education, State of Mexico Campus, Atizapan de Zaragoza, Mexico

Original scientific paper
https://doi.org/10.2298/TSCI151218311O

In this work, we study the liquid-solid interface dynamics for large time intervals on a 1-D sample, with homogeneous Neumann boundary conditions. In this kind of boundary value problem, we are able to make new predictions about the interface position by using conservation of energy. These predictions are confirmed through the heat balance integral method of Goodman and a generalized non-classical finite difference scheme. Since Neumann boundary conditions imply that the specimen is thermally isolated, through well stablished thermodynamics, we show that the interface behavior is not parabolic, and some examples are built with a novel interface dynamics that is not found in the literature. Also, it is shown that, on a Neumann boundary value problem, the position of the interface at thermodynamic equilibrium depends entirely on the initial temperature profile. The prediction of the interface position for large time values makes possible to fine tune the numerical methods, and given that energy conservation demands highly precise solutions, we found that it was necessary to develop a general non-classical finite difference scheme where a non-homogeneous moving mesh is considered. Numerical examples are shown to test these predictions and finally, we study the phase transition on a thermally isolated sample with a liquid and a solid phase in aluminum.

Key words: *Stefan problem, Neumann boundary problem, heat balance, finite difference method*

Introduction

A two-phase Stefan problem is a moving boundary problem where a solution to the diffusion equations in each phase is desired, and the motion of the interface is unknown. In this class of problems, the motion of the interface demands the use of numerical methods to find an approximate solution, due to the non-linearity of the problem introduced by the phase transition. When solving the Stefan problem on a finite bar, if the system is thermally isolated, the interface moves according to conservation of energy. For example, when the system reaches thermodynamic equilibrium, the interface stops moving because all the internal energy has been transferred to melt the solid. This happens for long values of time, where the interface approaches asymptotically to a given position that depends on the energy, which is an input to the system, through the initial temperature profile. Most authors, study the behavior of the in-

* Corresponding author, e-mail: j.a.otero@itesm.mx

terface for small time values, finding solutions by using finite difference methods [1-8] or semi--analytical approaches [9-12], where it is possible to compare the obtained numerical solution with the exact analytical solution [1, 2, 6] for a semi-infinite bar, because in this time regime the behavior is parabolic and the exact solution provides a tool for validation of the solutions. However, there is no information in the literature that explains the dynamics of the interface at larger time values. For example, in [2], without further discussions, the authors mention that the difference between their numerical solutions and the exact analytical solution for large times is due to finite size effects.

For the Dirichlet boundary conditions problem [13], the time behavior of the interface is far from being parabolic at large values of time, and one of the physical implications of these type of boundary conditions, is that temperature profiles within each phase of the specimen and the interface position at large time values, are completely independent of the initial temperature profile. By using Neumann boundary conditions, the physical picture changes drastically, since in this case, the solution of the problem depends completely on the initial temperature profile, due to conservation of energy. The goal of this work is to show that the interface motion is not parabolic as in the Dirichlet boundary value problem [13], and show that in this case, the solution depends entirely on the initial temperature profile. Even more, since energy conservation must be satisfied at every time step of the simulation, we developed a generalization of the non-classical finite difference scheme (NC-FDS). Also a generalized version of the heat balance integral method (HBIM) is used, in order to consider several temperature profiles and show that the numerical methods are in perfect agreement with our predictions. Some results obtained from numerical experiments are shown and compared with the predicted interface position and finally, we compare these predictions with solutions obtained from the general HBIM and NC-FDS in aluminum.

Statement of the problem

We consider a sample of size, L, prepared with liquid and solid phases of a pure substance, where the liquid-solid interface is initially at some position, ξ, and has a temperature equal to the fusion temperature, T_f. It will be assumed that each medium has a temperature profile $T_1(x,t)$ and $T_2(x,t)$ for liquid and solid phases, respectively. The temperature at any point within the liquid phase, is above T_f and within the solid phase is below T_f. In this work, we consider temperature profiles with homogeneous Neumann boundary conditions:

$$\left.\frac{\partial T_1(x,t)}{\partial x}\right|_{x=0} = 0, \quad \left.\frac{\partial T_2(x,t)}{\partial x}\right|_{x=L} = 0 \tag{1}$$

and an homogeneous Dirichlet boundary condition at the interface:

$$T_1(\xi,t) = T_2(\xi,t) = T_f \tag{2}$$

where the sub index 1 (2) represents liquid (solid) phase and L is the size of the specimen. Equation (1), means that the bar is thermally isolated from the surroundings which imply that energy is only transferred between the liquid and solid phases. These boundary conditions demand energy conservation, and as we will show later, this implies that the resulting interface position depends on the initial temperature profile. For this reason, several temperature profiles will be considered:

$$T_i(x,0) = f_i(x), \quad i = 1, 2 \tag{3}$$

where $f(x)$ can be obtained in order to satisfy the boundary conditions given by eq. (1), with $\xi(0) = B$, and $B > 0$. To find the solution of the heat equations in each phase, it will be assumed

that the thermodynamic variables do not depend on the temperature. Therefore, the heat equation in each medium is written:

$$\frac{\partial T_i}{\partial t} = \alpha_i \frac{\partial^2 T_i}{\partial x^2}, \text{ with } (i-1)\xi \le x \le (2-i)\xi + (i-1)L \tag{4}$$

where $\alpha_i = k_i/\rho_i C_i$ is the heat diffusion coefficient, with heat capacity, C_i, density, ρ_i, and thermal conductivity, k_i, at each phase i, and the Stefan condition (SC) describing the motion of the interface:

$$\rho_i L_f \frac{\mathrm{d}\xi}{\mathrm{d}t} = k_2 \left.\frac{\partial T_2}{\partial x}\right|_{x=\xi^+} - k_1 \left.\frac{\partial T_1}{\partial x}\right|_{x=\xi^-} \tag{5}$$

where L_f is the latent heat of fusion and ρ_1 (ρ_2) is the density of the liquid (solid) phase.

Numerical solutions

Since the Neumann boundary value problem implies that the total energy of the system must be conserved, the NC-FDS has been generalized in order to satisfy energy conservation at every time interval. In this NC-FDS we will consider a non-homogeneous mesh within each phase.

Non-classical finite difference scheme for a non-homogeneous moving mesh

An implicit scheme is used, therefore, the partial time derivative of the temperature is expressed as a first order approximation of the backward difference in time:

$$\frac{\partial T_i}{\partial t} \approx \frac{{}^{m,n}T_i - {}^{m,n-1}T_i}{\Delta t} \tag{6}$$

where Δt represents the length of the time step. The discretization of the position x, is represented by m and the discretization of time, t, is represented by n. Therefore, in this notation, ${}^{m,n}T_i = T_i(x_m, t_n)$. Generalization of the NC-FDS over a non-homogeneous mesh is done by adding the Taylor expansions for ${}^{m+1,n}T_i$ and ${}^{m-1,n}T_i$ up to fourth order in Δx_i by using a step size of different length to the right as $\Delta x_{R_i} = {}^{m+1,n}x_i - {}^{m,n}x_i$, and $\Delta x_{L_i} = {}^{m,n}x_i - {}^{m-1,n}x_i$ to the left. Keeping in mind that ${}^{m,n}T_i^{(j)} = \partial^j T_i(x_m, t_n)/\partial x^j$, we obtain:

$$\frac{{}^{m+1,n}T_i}{\Delta x_{R_i}} + \frac{{}^{m-1,n}T_i}{\Delta x_{L_i}} = {}^{m,n}T_i\left(\frac{1}{\Delta x_{R_i}} + \frac{1}{\Delta x_{L_i}}\right) + \frac{1}{2}{}^{m,n}T_i^{(2)}(\Delta x_{R_i} + \Delta x_{L_i}) +$$
$$+ \frac{1}{6}{}^{m,n}T_i^{(3)}(\Delta x_{R_i}^2 - \Delta x_{L_i}^2) + \frac{1}{24}{}^{m,n}T_i^{(4)}(\Delta x_{R_i}^3 + \Delta x_{L_i}^3) + \cdots \tag{7}$$

Using a more general central difference definition, which applied to the fourth derivative, is written as:

$${}^{m,n}T_i^{(4)} = \frac{2}{\Delta x_{R_i} + \Delta x_{L_i}}\left(\frac{{}^{m+1,n}T_i^{(2)} - {}^{m,n}T_i^{(2)}}{\Delta x_{R_i}} - \frac{{}^{m,n}T_i^{(2)} - {}^{m-1,n}T_i^{(2)}}{\Delta x_{L_i}}\right) + o(\Delta x_{R_i}^2, \Delta x_{L_i}^2) \tag{8}$$

The key to obtain the NC-FDS that can be used over a non-homogeneous mesh, is to find an expression for the third derivative in terms of the second derivative. We substitute the

previous equation and the expression for the third derivative on eq. (7) to obtain an equation in terms of second derivatives. Next, every term where the second derivative appears, is replaced by the discretized heat equation, and after simplification of the resulting expression, we obtain a more general model of six points that can be solved over a non-homogeneous mesh:

$$\left[\gamma_i^{(L)} - \lambda_i^{(L)}\right]^{m-1,n} T_i + \left(2\lambda_i + \frac{5}{6}\right)^{m,n} T_i + \left[\gamma_i^{(R)} - \lambda_i^{(R)}\right]^{m+1,n} T_i =$$

$$= \gamma_i^{(L)\ m-1,n-1} T_i + \frac{5}{6}{}^{m,n-1} T_i + \gamma_i^{(R)\ m+1,n-1} T_i \tag{9}$$

where we have defined:

$$\lambda_i = \frac{\alpha_i \Delta t}{\Delta x_{R_i} \Delta x_{L_i}}, \quad \lambda_i^{(L)} = \frac{2\alpha_i \Delta t}{\Delta x_{L_i}\left(\Delta x_{R_i} + \Delta x_{L_i}\right)}, \quad \lambda_i^{(R)} = \frac{2\alpha_i \Delta t}{\Delta x_{R_i}\left(\Delta x_{R_i} + \Delta x_{L_i}\right)}$$

and

$$\gamma_i^{(L)} = \frac{2\Delta x_{L_i} - \Delta x_{R_i}}{6(\Delta x_{R_i} + \Delta x_{L_i})}, \quad \gamma_i^{(R)} = \frac{2\Delta x_{R_i} - \Delta x_{L_i}}{6(\Delta x_{R_i} + \Delta x_{L_i})}$$

With the previous definitions, by setting $\Delta x_{R_i} = \Delta x_{L_i}$ on eq. (9), we can obtain the six-point model for a homogeneous mesh. In general, for a non-homogeneous mesh, the fourth order approximation to the derivatives that appear in eq. (1) and in the SC, eq (5) is given by:

$${}^{m,n}T_2^{(1)} = \frac{1}{12\Delta x_{R_2}}(-25\,{}^{m,n}T_2 + 48\,{}^{m+1,n}T_2 - 36\,{}^{m+2,n}T_2 + 16\,{}^{m+3,n}T_2 - 3\,{}^{m+4,n}T_2) \tag{10}$$

and

$${}^{m,n}T_1^{(1)} = \frac{1}{12\Delta x_{L_1}}(25\,{}^{m,n}T_1 - 48\,{}^{m-1,n}T_1 + 36\,{}^{m-2,n}T_1 - 16\,{}^{m-3,n}T_1 + 3\,{}^{m-4,n}T_1) \tag{11}$$

Heat balance integral method

In this section, we generalize the HBIM as in [10], in order to consider several temperature profiles. In general, we represent the temperature profile:

$$T_i(x,t) = a_i\left(\xi - x\right) + b_i\left(\xi - x\right)^n + T_f, \text{ with } (i-1)\xi \le x \le (2-i)\xi + (i-1)L \tag{12}$$

where n must be equal or greater than 2, in order to satisfy the boundary conditions given by eqs . (1) and (2). As usual, a_i and b_i with $i = 1,2$ for mediums 1 and 2, are functions of time. To obtain the initial profile, the values of a_i and b_i at $t = 0$ second, with $i = 1,2$, are determined by substitution of eq. (12) into eq. (1) and setting the initial temperature at each side of the specimen as $T_1(0,0) = T_l$ for the liquid phase and $T_2(L,0) = T_s$ for the solid phase. After applying Neumann boundary conditions to these profiles, the following relations between the functions a_i and b_i are obtained for the liquid and solid phases:

$$a_1 + nb_1\xi^{n-1} = 0 \quad \text{and} \quad a_2 + nb_2\left(L - \xi\right)^{n-1} = 0 \tag{13}$$

After substitution of eq. (12) in the SC, eq. (5), the resulting equation has the form:

$$\rho_i L_f \frac{\mathrm{d}\xi}{\mathrm{d}t} = k_1 a_1 + k_2 a_2 \tag{14}$$

Integrating the diffusion equation in medium 1, from $x = 0$ to $x = \xi$, and in a similar manner, integrating the diffusion equation in medium 2, from $x = \xi$ to $x = L$, the following set of ODE in time are obtained:

$$\frac{1}{n+1}\frac{\mathrm{d}b_i}{\mathrm{d}t}\zeta_i^n + \frac{\mathrm{d}\zeta_i}{\mathrm{d}t}(b_i\zeta_i^{n-1} + a_i) + \frac{1}{2}\frac{\mathrm{d}a_i}{\mathrm{d}t}\zeta_i - n\alpha_i b_i \zeta_i^{n-2} = 0 \tag{15}$$

with $\zeta_1 = \xi$ in medium 1, and $\zeta_2 = L - \xi$ in medium 2. Solving for a_1 and a_2 from eq. (13) and substitu ting in eqs. (14) and (15) we obtain a set of three ODE in time for the functions b_i and ξ that can be solved with the initial temperature profile.

Results and discussion

In this section, the finite difference solutions for several examples will be obtained and compared with the approximate analytical solutions for large time intervals. These solutions will be validated with the predicted asymptotic behavior of the interface, that can be obtained by using conservation of energy. This asymptotic value, will be used in every numerical experiment presented in this section, to fine tune the solutions obtained from the NC-FDS and the HBIM. Every numerical experiment will be designed so that the temperature at thermodynamic equilibrium of the entire specimen is equal to T_f. For the Neumann boundary value problem, the change in internal energy of the system must be equal to the energy needed for the phase transition. Using the change of internal energy at any given position:

$$\mathrm{d}U_1(x) = \mathrm{d}m_1 C_1[T_{\mathrm{eq}} - T_1(x,0)] \quad \text{and} \quad \mathrm{d}U_2(x) = \mathrm{d}m_2 C_2[T_{\mathrm{eq}} - T_2(x,0)] \tag{16}$$

where $\mathrm{d}m_1 = \rho_1 A\mathrm{d}x$ and $\mathrm{d}m_2 = \rho_2 A\mathrm{d}x$ for the liquid (solid) phases. Next, we integrate the previous equations to obtain the total change in internal energy ΔU. For an isolated system, the change in internal energy is used only for the phase transition, $\Delta U = A\rho_i(\xi_{\mathrm{eq}} - \xi)L_f$, where the value of ξ is the initial position of the interface. From this, we can find an exact expression for the position of the interface at thermodynamic equilibrium, ξ_{eq}. By using the initial temperature profiles shown in eq. (12), the expression for any value of n, in case of a melting process is:

$$\xi_{\mathrm{eq}} = \xi + \frac{\rho_1 C_1}{\rho_2 L_f}\left(\frac{a_1}{2}\xi^2 + \frac{b_1}{n+1}\xi^{n+1}\right) + \frac{C_2}{L_f}\left[\frac{a_2}{2}(L-\xi)^2 + \frac{b_2}{n+1}(L-\xi)^{n+1}\right] \tag{17}$$

where it is assumed that $T_{\mathrm{eq}} = T_f$, and for a solidification process:

$$\xi_{\mathrm{eq}} = \xi + \frac{C_1}{L_f}\left(\frac{a_1}{2}\xi^2 + \frac{b_1}{n+1}\xi^{n+1}\right) + \frac{\rho_2 C_2}{\rho_1 L_f}\left[\frac{a_2}{2}(L-\xi)^2 + \frac{b_2}{n+1}(L-\xi)^{n+1}\right] \tag{18}$$

Let us keep in min d that eqs. (17) and (18) were derived from the initial temperature profiles that appear in eq. (12), therefore, the interface position, ξ, and the values of the functions a_i and b_i at medium i are evaluated at $t = 0$ second. It is important to note that, just by using Neumann boundary conditions, we obtain eqs. (17) and (18), which are of completely different nature than the interface position in the asymptotic limit, for a Dirichlet boundary value problem [13]. Even more, for a Dirichlet boundary value problem, the asymptotic interface position only depends on the thermal conductivities of each phase [13], on the other hand, for the Neumann boundary value problem, the interface position for long time intervals depends on the densities, specific heat capacities and latent heat of fusion. We will illustrate a few examples where the non-parabolicity of the interface dynamics is evident, but we will also show by

using the NC-FDS and HBIM, that the interface position strongly depends on the shape of the initial temperature profile, as predicted by eqs. (17) and (18).

For the first part of the discussion, we will set the thermodynamic variables of density and specific heat, equal to one and the fusion temperature will be taken as $T_f = 0$. As in [2], the diffusivity is reduced to $\alpha_1(\alpha_2) = k_1(k_2)$ for the liquid (solid) phase. In this system of units, the SC and diffusion equations are simplified correspondingly [2]. All examples presented in this part of the results are obtained from the solution of the simplified diffusion equations and the SC over a specimen of length $L = 1.0$, and the time increment for the finite difference simulations is $\Delta t = 2.5 \cdot 10^{-4}$.

In fig. 1 we show the results from two numerical experiments. On fig. 1(a), the initial profile in each phase was obtained by using $\xi = 0.6$, $T_l = 0.8$, and $T_s = -1.0$. Initial values of $\xi = 0.4$, $T_l = 1.0$, and $T_s = -0.8$ were used to obtain the results shown in fig. 1(b). By using these initial conditions and eq. (1), the values of a_i and b_i at $t = 0$ can be obtained in each case. By setting the densities and specific heat capacities equal to one in eqs. (17) and (18) we can obtain the position of the interface at thermodynamic equilibrium, which is also shown in fig. 1. Through eqs. (17) and (18), we have designed the experiments in order to reach a desired interface position at thermodynamic equilibrium. We have also chosen the initial interface position so that for small times, the net flux through the interface produces solidification for the example shown in fig. 1(a) and melting for the case shown in fig. 1(b). The experiment was designed this way to show the precision of the numerical and semi-analytical methods by comparing the results with the predicted interface position, and also to demonstrate that even for small time intervals, we can find cases where the interface dynamics is not parabolic. The non-parabolicity of ξ for small time intervals in the example shown in fig. 1 is a consequence of the boundary conditions imposed on the specimen, and this is a particular behavior that can not be observed in a Dirichlet boundary value problem [13].

Non-parabolic behavior close to thermodynamic equilibrium in aluminum

Here we will discuss the consequences of eqs. (17) and (18) for the phase transition on a thermally isolated specimen of $L = 1.0$ m containing a liquid-solid interface in pure aluminum. We will use the same thermodynamic variables as in [6], which will be assumed to be independent of the temperature. For the liquid phase, $k_1 = 215$ W/mK, $\rho_1 = 2380$ kg/m^3, and $C_1 = 1130$ J/kgK. For the solid phase, $k_2 = 225.5$ W/mK, $\rho_2 = 2545$ kg/m^3, and $C_2 = 1016$ J/kgK. A latent heat of fusion of $L_f = 396 \cdot 10^3$ J/kg and fusion temperature $T_f = 933.52$ K are used in the shown examples. Figure 2 illustrates the resulting interface motion for an initial temperature profile with $n = 3$, obtained with the NC-FDS and the HBIM. For the example shown in fig. 2(a) the initial position of the interface is $\xi = 0.60$ m, the initial temperature at $x = 0$ m is $T_l = 1020$ K, and at $x = L$, the initial temperature is $T_2 = 525.25$ K. The time step used by the NC-FDS was 0.10 second, and it was solved by using a moving non-homogeneous mesh with $N_1 = 720$ nodes on the liquid side and $N_2 = 480$ nodes on the solid part of the specimen. As observed in fig. 2(a), the solution obtained from the NC-FDS and HBIM capture the long time behavior predicted by eq. (18), where we show the results for the first $1 \cdot 10^4$ s of simulation.

Figure 2(b) illustrates the dynamics of the interface obtained from an experiment, designed to show the predicting power of eq. (17). In this case, initial values of $\xi = 0.40$ m, $T_l = 1173$ K, and $T_s = 873.25$ K were used on an initial temperature profile with $n = 3$. With these values, and the boundary conditions given by eq. (1), it is possible to find a_i and b_i at each phase i, in order to obtain the position of the interface at thermodynamic equilibrium, ξ_{eq}, ac-

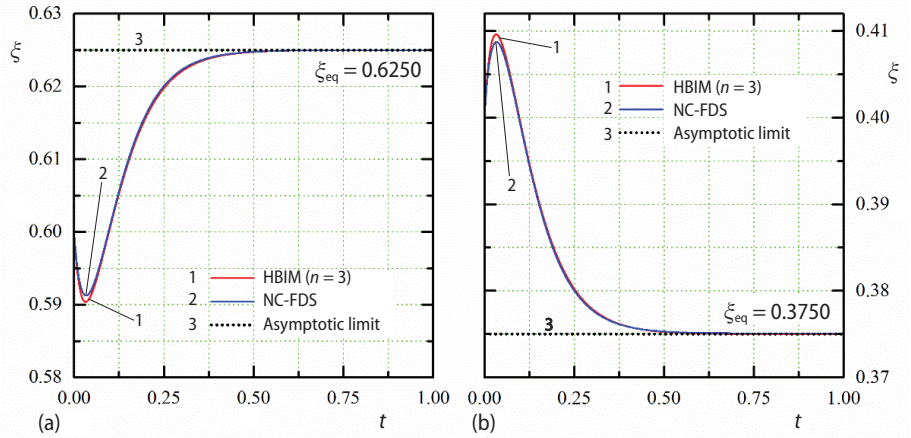

Figure 1. Interface motion for an initial temperature profile of the form given by eq. (12) with $n = 3$, a fusion point of $T_f = 0$ and a latent heat of fusion $L_f = 2.0$; interface dynamics with (a) $k_1 = 2.0$, $k_2 = 1.5$ and an initial interface position of $\xi = 0.6$, (b) $k_1 = 1.5$, $k_2 = 2.0$ and the initial position of the interface is $\xi = 0.4$

cording to eq. (17). This value is shown on fig. 2(b), and tested against the NC-FDS and HBIM. For this example, the NC-FDS was solved over a non-homogeneous mesh with $N_1 = 480$ and $N_2 = 720$ nodes with the same time step of 0.10 second. In this example, the initial temperature profile at each phase was chosen, so the loss of internal energy by the liquid phase is greater than the internal energy absorbed by the solid phase. In this situation the extra energy lost by the liquid is used to melt a section of solid, so eq. (17) predicts exactly the amount of liquid and solid that will remain on the sample at thermodynamic equilibrium. As shown in fig. 2(b), the NC-FDS and HBIM are observed to capture the behavior just discussed.

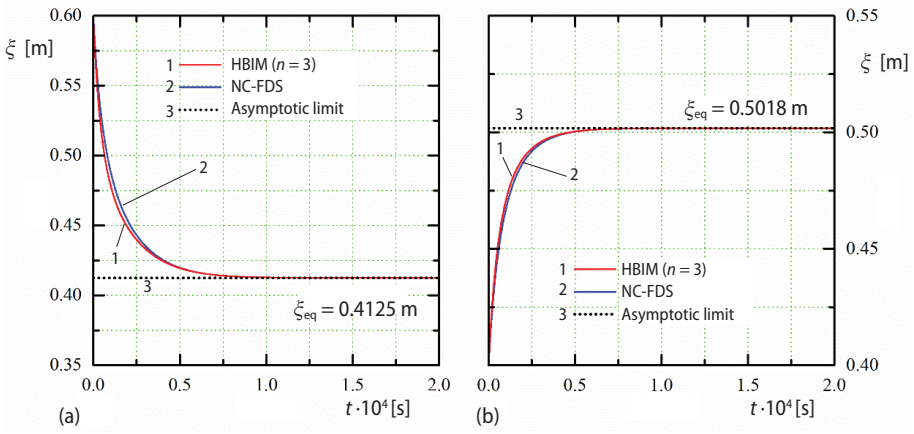

Figure 2. Interface motion for aluminum on a specimen of $L = 1.0$ m, with an initial temperature profile of the form given by eq. (12), with $n = 3$; initial conditions are chosen to observe (a) solidification of liquid aluminum, according to eq. (18), and (b) melting of solid aluminum according to eq. (17)

Finally, we show two examples where several temperature profiles are used in order to show that for the Neumann boundary value problem, the results are highly dependent on the shape of the profile, contrary to the expected behavior of the interface in a Dirichlet boundary value problem, where the resulting interface position for long time intervals, is completely independent of the initial temperature profile [13]. Figures 3(a) and 3(b) show the resulting interface dynamics obtained with the NC-FDS, for the same temperatures T_l, T_s and initial interface position of the previous example, but using different values of n for the temperature profiles given by eq. (12). The results shown in fig. 3 also consider a step-like temperature profile, where the temperature in the liquid and solid regions of the specimen are constant functions of the position, and equal to T_l (T_s) for the liquid (solid) phases. For the step-function like profile shown in fig. 3(a), $N_1 = 720$ and $N_2 = 480$ were used. In fig. 3(b) we used $N_1 = 480$ and $N_2 = 720$ nodes for the step-function like profile. By calculating the change of internal energy in the system, it is straightforward to find the position of the interface at thermodynamic equilibrium as well. For a melting process, ξ_{eq} is given by:

$$\xi_{eq} = \xi + \left(\frac{\rho_1 C_1}{\rho_2 L_f}\right)\xi(T_l - T_f) + \frac{C_2}{L_f}(L - \xi)(T_s - T_f) \tag{19}$$

and for a solidification process:

$$\xi_{eq} = \xi + \frac{C_1}{L_f}\xi(T_l - T_f) + \left(\frac{\rho_2 C_2}{\rho_1 L_f}\right)(L - \xi)(T_s - T_f) \tag{20}$$

The NC-FDS is observed to capture the asy mptotic behavior predicted by eqs. (17)-(20), where the obtained motion of the interface is highly dependent on the initial temperature profile.

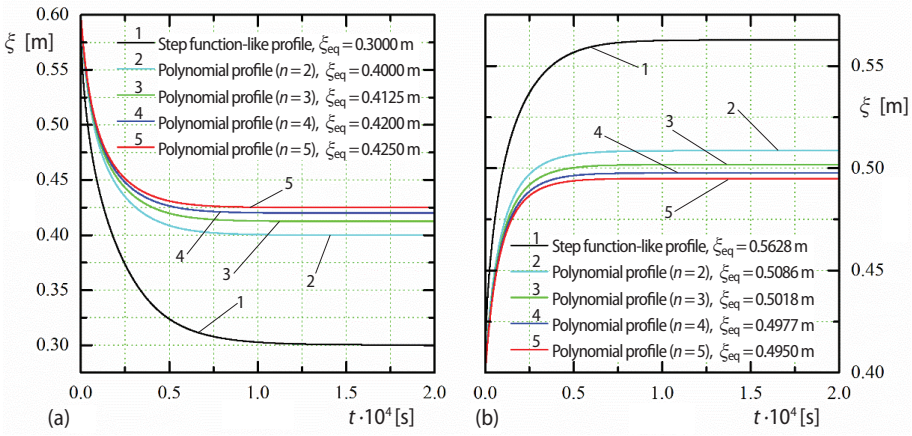

Figure 3. Interface motion for aluminum obtained with the NC-FDS over different polynomial profiles and for a step-like profile (a) Solidification of liquid aluminum with $T_l = 1020$ K and $T_s = 525$ K and (b) Melting of solid aluminum with $T_l = 1173$ K and $T_s = 873.25$ K; thermodynamic equilibrium values of the interface position according to eq. (17)-(20) are also shown for comparison with the numerical solution

Conclusions

In this work, we have found for the Stefan problem with homogeneous Neumann boundary conditions, general results about the dynamics of the phase transition within the sample that are not reported in the literature, and provide a wider understanding on the Stefan class of problems.

- By using conservation of energy, non-parabolic motion of the interface close to thermodynamic equilibrium is predicted.
- The initial conditions on the system and the nature of the boundary conditions, can give rise to examples, where non-parabolicity of the interface dynamics can also be observed at small time intervals.
- By using eq. (17), it is possible to design an experiment where a section of solid is melted at thermodynamic equilibrium. However, by using heat transport, the initial position of the interface may be chosen in order to obtain a net flux that produces solidification of liquid for small times.
- By using eq. (18) and heat transport, we can design experiments with an opposite effect to the aforementioned example.
- According to eqs. (17)-(20), the position of the interface can be predicted exactly and numerical methods can be fine-tuned and developed in order to capture the physics predicted by these equations.
- On a thermally isolated system, the main physics that governs the dynamics of the interface, is conservation of energy. Therefore, the longtime behavior of the interface, strongly depends on the densities, specific heat capacities at each phase and the latent heat of fusion, as predicted by eqs. (17)-(20).
- Since the system is thermally isolated and the initial temperature profile is related with the amount of total energy, contrary to a Dirichlet boundary value problem, the resulting position of the interface at thermodynamic equilibrium depends highly on the shape of the profile, as shown by eqs. (17)-(20).
- The generalized NC-FDS and HBIM are observed to capture the predicted position of the interface at thermodynamic equilibrium.

References

[1] Javierre-Perez, E., Literature Study: Numerical Problems for Solving Stefan Problems. Report No. 03-16, Delf University of Technology, Delft, The Netherlands, 2003
[2] Javierre, E., *et. al.*, Comparison of Numerical Models for One-Dimensional Stefan Problems, *J. Comput. Appl. Math.*, *192* (2006), 2, pp. 445-459
[3] Mitchell, S. L., Vynnycky, M., On the Numerical Solution of Two-Phase Stefan Problems with Heat-Flux Boundary Conditions, *J. Comput. Appl. Math.*, *264* (2014), July, pp. 49-64
[4] Mitchell, S. L., Vynnycky, M., Finite-Difference Methods with Increased Accuracy and Correct Initialization for One-Dimensional Stefan Problems, *Appl. Math. Comput.*, *215* (2009), 4, pp. 1609-1621
[5] Tadi, M., A Four-Step Fixed-Grid Method for 1D Stefan Problems, *J. Heat Transf.*, *132* (2010), 11, pp. 114502-114505
[6] Wu, Z.-C., Wand, Q.-C., Numerical Approach to Stefan Problem in a Two-Region and Limited Space, *Thermal Science*, *16* (2012), 5, pp. 1325-1330
[7] Esen, A., Kutluay, S., A Numerical Solution of the Stefan Problem with a Neumann-Type Boundary Condition by Enthalpy Method, *Appl. Math. Comput.*, *148* (2004), 2, pp. 321-329
[8] Caldwell, J., Kwan, Y. Y., Numerical Methods for One-Dimensional Stefan Problems, *Commun. Numer. Meth. Engng.*, *20* (2004), 7, pp. 535-545
[9] Goodman, T. R., Application of Integral Methods to Transient Nonlinear Heat Transfer, Advances in Heat Transfer, Academic Press, New York, USA, 1964

[10] Fraguela, A., *et. al.*, An Approach for the Identification of Diffusion Coefficients in the Quasi-Steady State of a Post-Discharge Nitriding Process, *Math. Comput. Simulat.*, *79* (2009), 6, pp. 1878-1894
[11] Mitchell, S. L., Myers, T. G., Application of Standard and Refined Heat Balance Integral Methods to One Dimensional Stefan Problems, *SIAM Rev.*, *52* (2010), 1, pp. 57-86
[12] Sadoun, N., *et. al.*, On the Goodman Heat-Balance Integral Method for Stefan Like-Problems, *Thermal Science*, *13* (2009), 2, pp. 81-96
[13] Hernandez, E. M., *et. al.*, Non Parabolic Interface Motion for the One-Dimensional Stefan Problem: Dirichlet Boundary Conditions, *Thermal Science*, *21* (2017), 6A, pp. 2321-2330

Paper submitted: December 18, 2015
Paper revised: November 29, 2016
Paper accepted: December 3, 2016